



# Loose Ash Fills Reinforced With the High Confined Encased Stone Columns: Experimental and Numerical Investigation

Sudheer Kumar Jala · Saurabh Rawat · Ashok Kumar Gupta

Received: 4 December 2019 / Accepted: 12 November 2020 / Published online: 20 November 2020  
© Springer Nature Switzerland AG 2020

**Abstract** The use of industrial waste (ash) in large-scale earthworks for civil engineering applications such as construction of highway embankments, the rise of ash dykes, the filling low-lying areas, fillings of buildings, solves the problem of waste disposal besides in addition to the conservation of the natural soils. It has a low density, low consolidation, lower potential for bearing and higher settlement. To use these areas for construction purposes, it is necessary to reinforce them at deeper depths. The present study uses highly confined stone columns to investigate the strengthening of ash fills. A total of six cases are investigated, including slope reinforced with an encased stone column. Model tests were conducted with pond ash at 40% relative density with a circular footing on untreated and treated ash fills. The enhanced cases include ordinary stone columns, vertically encased columns with geotextile, vertically encased columns with geogrid, highly confined vertically encased columns with both geotextile and geogrids (HC-1) and highly encased columns with both vertical encased geotextile and horizontal geogrid (HC-2) layers. The parametric study includes an examination of load-settlement behavior, load-

carrying ratio, settlement reduction ratio, and stiffness factor, modulus of subgrade reaction and post-failure behavior of slopes reinforced with encased stone columns. In all cases, the high confined encased system yields better results. In each case, the stone column failure pattern of was observed at a distance range of 1–3 times the stone column diameter. Post-failure behavior indicates that for steep slopes where massive slip failures are expected, highly confined encased stone columns can be useful. Results are validated by the numerical modelling analysis of Plaxis.

**Keywords** Stone columns · Geotextile · Geogrid · Stiffness · Modulus of subgrade reaction · Load carrying capacity (LCR)

## 1 Introduction

At present, nearly 184.14 million tons of coal ash is being produced annually in India and more than 70,000 acres of land are presently occupied by ash ponds. The use of ash in various applications in civil engineering such as brick making, cement, concrete, and soil stabilization has been doing, and it is recognized. In India fifty nine cities municipal solid waste occupies the 9233 sq.km of land, height of the dumps vary from 3 m to several meters. The maximum constitution of municipal solid waste at produces

---

S. K. Jala (✉) · S. Rawat · A. K. Gupta  
Department of Civil Engineering, Jaypee University of  
Information Technology, Solan, HP, India  
e-mail: sudheeritd@gmail.com

S. Rawat  
e-mail: saurabhdec19@gmail.com

sources and collection points was discovered on a wet weight basis and it consists mainly of large biodegradable matter is (40–60%), ash and fine earth (30–40%), paper (3–6%) and glass and metals (less than 1%) (Sharholly et al. 2008). This poses a two-way threat to the society that is land scarcity and the other dumps exposed to the atmosphere poses environmental problems.

These unscientific dump sites (landfills) have a low density, low shear strength and higher settlement that makes maximum dumped area is worthless. It can be utilized once these sites are improved in geotechnical engineering properties; thereby they may allow for low weight structures, constructing parks, parking areas, can be used as highway material, embankments and filling low-lying areas, etc.

Present times every unsuitable ground is forced to be utilized by treating them with different techniques such as dynamic compaction, deep compaction, vibrofloat compaction and by installation of sand/stone columns. Ash fills containing loosely compacted, low strength and a wide range of particles can be strengthened with granular columns at deeper depths (Greenwood 1970; Bairagi et al. 2012). Many researchers have attempted to improve the ash pond grounds with grouting curtains and prefabricated vertical drains (Gandhi 1996; Rao 2009).

## 2 Back Ground

Stone columns (SCs) reinforce the soft cohesive soils, improve load-carrying capacity and reduce the settlement (Hughes and Withers 1975). Ground improvement through SCs has been successful at the field level in case of soft, low compressible clays, and loose granular sands. Many researchers have experimentally and numerically conducted studies on SC's filled with natural aggregates of size 2–70 mm in clay soils, where undrained shear strength is less than 15 kPa (Naderi et al. 2018; Ghazavi et al. 2018; Cengiz and Guler 2018; Fattah et al. 2016; Ali et al. 2014; Ghazavi and Nazari 2013; Dash and Bora 2013; Murugesan and Rajagopal 2010; Gniel and Bouazaa 2009; Ambily and Gandhi 2007). SCs have also been reported useful in improving the load-carrying capacity of soft composite soil. SC's reduce the settlement, improve the modulus of subgrade reaction, and reduce liquefaction potential (Salem 2017) accelerate consolidation and

increase the stability of slopes (Vekli et al. 2012). SC's are vertically encased with geosynthetics to provide the lateral confinement has been studied using experimental investigation by (Malarvizhi and Illamparuthi 2007; Murugesan and Rajagopal 2010, Wu and Hong 2009, Ghazavi and Afshar 2013; Ali et al. 2014; Yoo et al. 2015; Miranda and Da Costa 2016; Gu et al. 2016; Fattah et al. 2016; Mohapatra et al. 2016; Debnath and Dey 2017; Das and Bhora 2013; Cengiz and Guler 2018). However, very few published literature is available on SCs reinforced with horizontal geogrid layers (Prasad and Satyanarayana 2016; Ghazavi et al. 2018). It is also observed from the literature that steel nails are also used to provide lateral stiffness to the granular columns (Shivashankar et al. 2010). Geosynthetic high confining encasement of aggregates column can be applied even in extremely soft soils with very low undrained shear strength less than 2 kPa (Alexiew et al. 2005). This encasement provides additional stiffness to the column, thereby increasing the load-carrying capacity.

The capacity of the SC is highly dependent on the strength of fill material, its compaction, drainage characteristics, and confining stress of the surrounding soil. Various materials other than conventional fill materials, such as sand and natural aggregates, are being used to fill SCs. The selection of filler material primarily depends on availability, suitability, and material cost. Previous researchers (Nazaruddin et al. 2013), have carried out studies on crushed stone pulverized fuel ash as filler material for SC's, Fly ash aggregates has also been employed by, studied tire chips as fill in SC's, (Ayothiraman and Soumya 2015; Prasad and Satyanarayana 2016) used silica–manganese slag, recycled aggregates by (Amini 2016), and coal bottom ash by (Hassan et al. 2015; Demir et al. 2016; Mazumder 2018) has also been tested as SC fill. The geogrid confined GESC's exhibit higher stress concentration ratio than OSC, lateral bulging controlled upto maximum stiffness (Gu et al. 2016). Relative densities of 50% and 80% two specimens were encased with geotextile tested in a triaxial cell result depicted that strength considerably improved (Miranda and Costa 2016). The effective spacing between columns was found to be 1.5d (d—diameter of column) (Fattah et al. 2016).

Prefabricated vertical drains are used in pond ash dykes to improve the bearing capacity and reduce larger settlement, thereby raising the height of the

dykes (Rao 2009). Floating stone columns (FSC's) length is greater than 5 times its diameter will not increase the bearing capacity. They filled with crushed bricks, recycled aggregates and natural aggregates partially increase the bearing capacity in soft clay soils (Dash and Bora 2013; Shahverdiand Haddad 2019).

Studies on clay slopes reinforced with OSC's and GESC's observed that the bearing capacity of a strip footing on GESC's found to be higher than ordinary stone columns (Naderi et al. 2018) with tiebacks increases the slope factor of safety (Hassan and Alturffy 2015). GESCs and OSCs exhibit better performance during and after seismic excitation, they worked as seismic energy breakers for liquefaction remediation (Cengiz.and Guler 2018; Salem et al. 2017).

The novelty of the present work can be realized from the limited literature on loose ash fills strengthening at a deeper depth using SCs.

From the literature study, it can be seen that many researchers have experimentally and numerically proved that SC's with and without encasement are efficient in soft clay soils, where undrained shear strength is less than 10–12 kPa. However, the lacunae are in regard to the less amount of work carried on the strengthening of pond ash fills with stone columns with and without encasement. The present study is carried on pond ash fills at a relative density of 40% columns filled with recycled concrete aggregates (RCA). The objectives of the study are determining load settlement behavior, load-carrying ratio (LCR), settlement reduction ratio (SRR), stiffness factor, modulus of subgrade and post-failure behavior of slopes encased with geogrid columns are investigated through six different cases of model tests conducted at 40% relative density. The following cases are presented in Table 1 and Fig. 1.

### 3 Experimental Investigation

#### 3.1 Materials

##### 3.1.1 Pond ash (PA) and Recycled Aggregates (RA)

Pond ash is collected from the thermal power plant, ROPAR, Punjab, India. The preliminary investigation is conducted as for the Bureau of Indian Standards (BIS) to understand the various geotechnical

properties of pond ash (PA) as tabulated in Table 2. The particle size distribution (BIS: 2720 (4)–1985) of pond ash depicts that 6.5% particles are greater than 2 mm, 2 mm–0.425 mm size particles are 20.5%, 0.425 mm–0.075 mm is 69.4% and less than 0.075 mm is 3.6% Fig. 2. The mean particle sizes and particle size index are also mentioned in Table 2. The coefficient of permeability (BIS: 2720 (17)–1986) is found to be 0.0086 cm/sec, compaction (BIS: 2720 (8)–1985) parameters obtain as 35% optimum moisture content and a maximum dry density is 10.2 kN/m<sup>3</sup>. Similar results are presented by Singh and Singh (2018), Trivedi and Sud (2007) and Reddy et al. (2018). The shear strength parameters obtained from the direct shear test (BIS: 2720 (13)–1986) yield cohesion of 0.33 kPa and an angle of internal friction of 32°. As the utility of conventional construction materials increases, natural aggregates have become more expensive and scarce. Alternatively, recycling of concrete is a relatively simple process where concrete cubes are broken and crushed in the material lab to convert into individual aggregates materials of the required quantity. Thus, recycled aggregates can be visualized as a solution to meet this ever-increasing demand for construction material. The particle size of the recycled aggregate is calculated by sieve analysis and is found to vary between 1 and 14 mm. The impact value of recycled aggregates is 14.45% which is classified as strong material BIS 2386 (part 4): 1963. The mean particle size along with its frictional properties is presented in Table 2 and Fig. 2.

##### 3.1.2 Geotextile

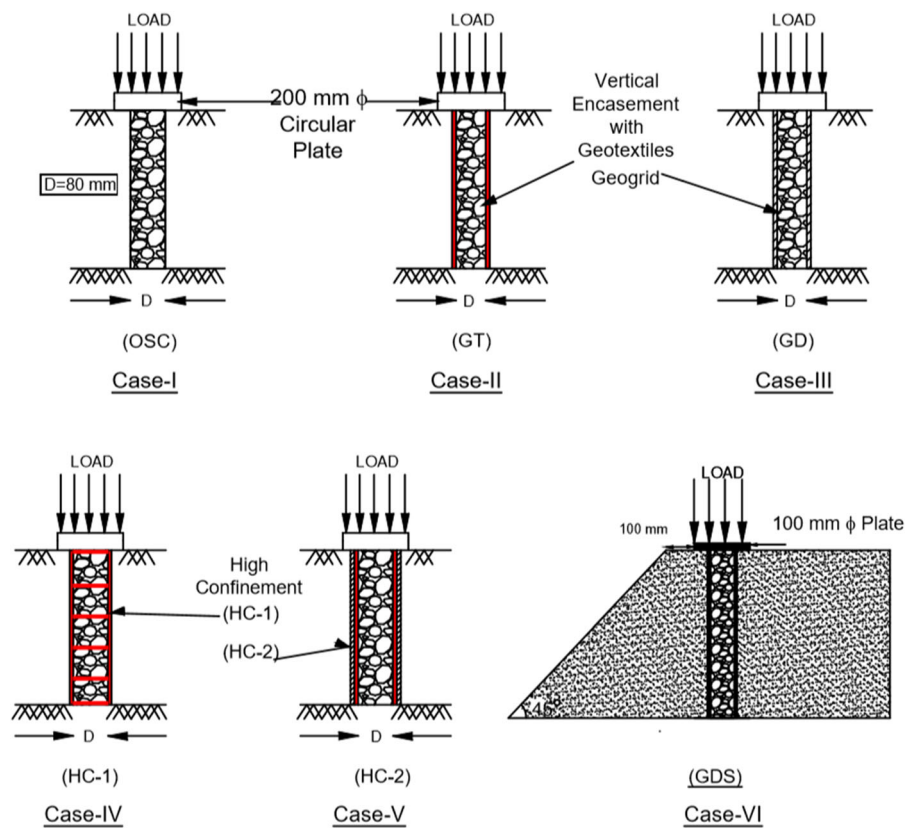
Non-woven geotextile used as encasement material to the column and it's the tensile strength is 6.8 kN/m. It works as a separator and filtration between the stones in the column and surrounding pond ash. Non-woven geotextile used three cases in this study, as refer to Fig. 1. Specification and photographs of geotextile are displayed in Table 3 and Fig. 3 respectively.

##### 3.1.3 Geogrid

Geogrids are made of polyester obtained from Strata geosystems India Pvt Ltd. It is other geosynthetic material used to encase the stone column in addition to geotextile. The tensile strength of the geogrid used in this is 33 kN/m. They are engineered to be

**Table 1** Cases studied and description code

Case no.	Description	Code
1	Ordinary stone columns in loose pond ash fill	OSC
2	Vertical encasement with geotextile	GT
3	Vertical encasement with geogrid	GD
4	Hybrid confinement i.e.combination of vertical geotextile encasement and horizontal geogrid layers in the column	HC-1
5	Hybrid confinement i.e.combination of vertically encased both geotextile and geogrid	HC-2
6	Slope reinforced with geogrid encased stone column (SC)	GDS

**Fig. 1** Schematic representation of cases studied (I–VI)

mechanically and chemically durable in both installation time and environmentally aggressive conditions. The geogrids are used in three cases they are vertically and horizontal discs refer Fig. 1. The Fig. 3 and Table 3 shows the specifications of the geogrid used in this study.

### 3.2 Experimental Methodology

A schematic test set up as shown in Fig. 4. The dimension of the tank is 1200 mm long, 1000 mm wide and 600 mm deep. The four sides and bottom of the tank were made of 6 mm thick mild steel plates and were stiffened laterally with steel angles on the outer surface to achieve essential stiffness against

**Table 2** Geotechnical properties of Pond ash (PA) and Recycled aggregates (RA)

Property	PA values	RA values
D <sub>10</sub> (mm)	0.2	4.75
D <sub>30</sub> (mm)	0.31	9.5
D <sub>60</sub> (mm)	0.43	14.51
C <sub>u</sub>	2.15	2.15
C <sub>c</sub>	1.12	1.12
Max. Dry density (kN/m <sup>3</sup> )	10.2	13.4
Min. Dry density (kN/m <sup>3</sup> )	7.7	11.2
Dry density (Kn/m <sup>3</sup> )	9.7	–
Optimum moisture content (%)	35	–
Coeff. of Permeability (cm/sec)	0.0086	–
Cohesion, c, (kN/m <sup>2</sup> )	0.33	0
Angle of Internal friction (φ) in (°)	32	44

**Table 3** Properties of biaxial Geogrid (SGi-040)

Aperture size	5 mm × 5 mm
Geogrid, 5% secant modulus (stiffness)	33.4 kN/m
Non woven geotextile, secant modulus	6.8 kN/m

thickness 25.4 mm and diameter is 200 mm. In the present study, all the cases the footing kept at the centre of the tank coincided with the centre of the stone column. The diameter of the footing is kept larger than the diameter of the stone column so that load fully occupies and loading application is on the composite bed (SC diameter and PA fill bed).

The load was applied through an automated hydraulic system. The load is transferred to the stone column measured by the electronic load cell of the capacity of 50 kN with a loading rate of 1 mm/min. There is a sensor attached to the hydraulic system that is connected to the data acquisition system that gives the load applied and vertical settlement of the footing. And also vertical dial gauges are attached diagonally opposite on the footing base to observe the vertical deformation.

### 3.2.1 Test Preparation

The tank size of 1200 mm × 1000 mm × 600 mm, PA filled in the tank using 425 micron sieve. Rainfall technique is used to fill and to achieve the required relative density. The tank was filled in 100-mm layers and replacement method was followed to make the stone column. PVC pipe selected to create a column in the PA bed. The open-ended pipe is driven into the PA bed at the central portion of the tank. In the case of OSC (ordinary stone column), PVC pipe is used as casing, recycled aggregates are filled inside the pipe and slowly lifted for every 50 mm. The tamping rod of 12 mm diameter is used to compact the aggregates in the column. In case of GESG (Geosynthetic encased stone column), geotextile wrapped around the pipe with an extra 100 mm overlap tied with the thread (Gniel and Bouazza 2010), the same procedure is followed for filling the aggregates in the column.

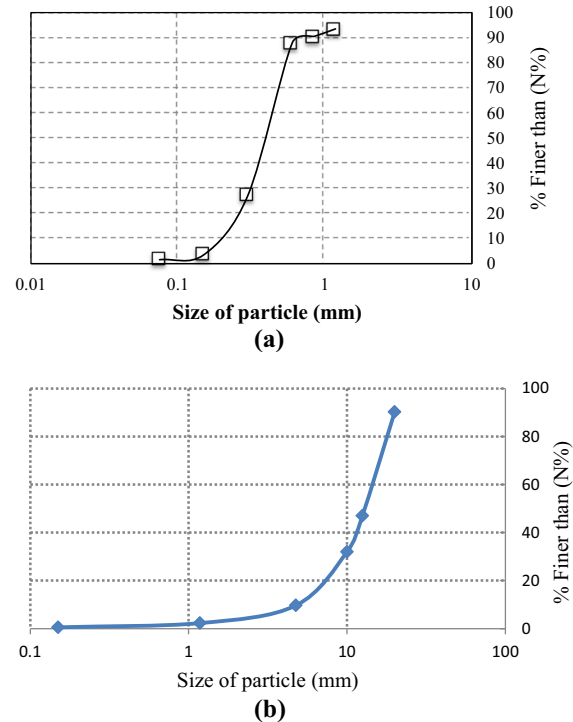


**Fig. 2** Particle size distribution of **a** pond ash, **b** recycled aggregates

bending during the tests. The tank inner surface walls were coated with silicon grease to minimize friction between the PA and the tank wall. The depth and size of the tank were certain to take care of the boundary effects. The circular footing was made of steel of

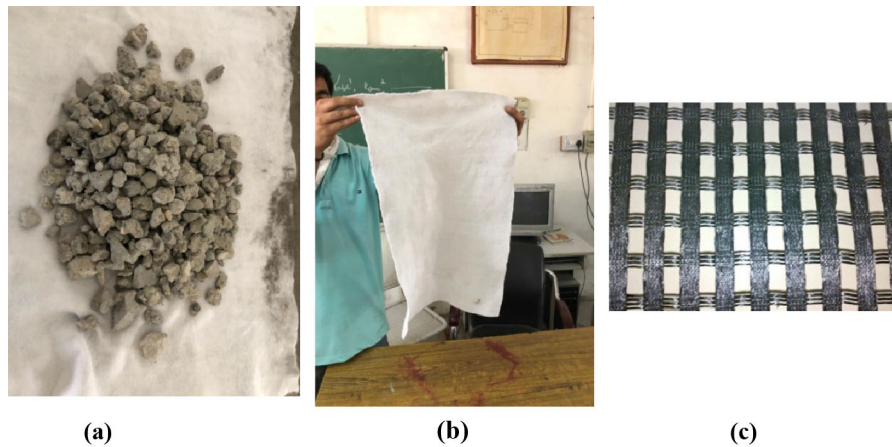


**Fig. 3** Material used for study **a** recycled aggregates, **b** geotextile, **c** geogrid

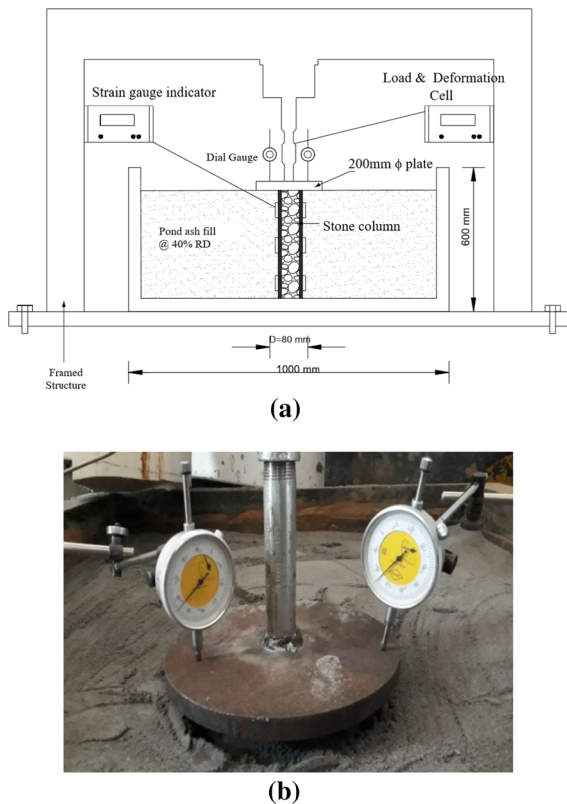


**Fig. 4** **a** Schematic diagram of the model test set up, **b** Photograph of the instrumentation with dial gauges

## 4 Results and Discussion

The laboratory experiments were performed primarily to determine the effect of some useful parameters on high confined encasement stone columns. The results

presented in the form of applied pressure–settlement, load-carrying ratio—settlement diameter of ratio, applied pressure–axial, lateral strain, modulus of subgrade reaction (stiffness) of the composite ground with the materials, etc. The test results of seven cases are presented in Table 4. From the seven cases, one of the studies is slope strengthening with the encased stone column.

### 4.1 High Encasement Effect on Load-Settlement

The result shows that the high confinement with the two different geosynthetics increases the load-carrying capacity of the stone column. The high confinement system that is HC-1, HC-2 bears the maximum load with a settlement of 50 mm. This is due to the high tensile modulus elasticity provided by the geotextile and geogrid. This high confinement system is much useful in loose-filled soils, lower consolidation, higher settlement, and lateral confinement can be much lower. Solid waste management dump sites and ash fill embankment.

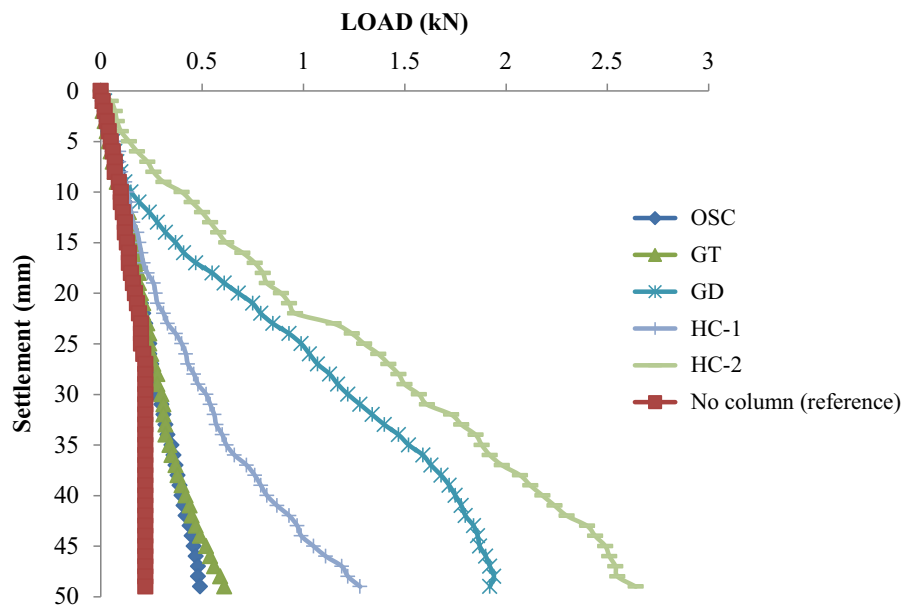
Load–settlement results presented in Fig. 5 the load-settlement behavior of single stone columns with a diameter of 80 mm with different types of confinement support system. From Fig. 5, all the cases of the stone column increase the ultimate load-carrying capacity of the composite ash fill compared to the pond ash alone, which is untreated. In all types of columns, the load-carrying capacity increases with the additional confinement support. The stone columns with a higher confinement system had shown the

**Table 4** Test results of cases studied

S. no	Type of composite ground/Encasement material	Load (N)	Applied stress (kPa)	Vertical settlement (mm)
1	Untreated (PA)	220 N	7 kPa	50 mm
2	OSC	490 N	15.6 kPa	50 mm
3	GT	610 N	19 kPa	50 mm
4	GD	1920 N	61.2 kPa	50 mm
5	HC-1	1280 N	40.7 kPa	50 mm
6	HC-2	2640 N	84 kPa	50 mm
7	GDS, slope (45°)	1190 N	152.6 kPa (100 mm dia.plate)	50 mm

OSC—ordinary stone column, GT—Geotextile, GD—Geogrid, HC-1—High confined

**Fig. 5** Variation of the load—settlement of stone column with different encasement



significant load-carrying capacity. This is due to the additional restriction provided to the column stones, in case of HC-1 the horizontal geogrid layers gives the additional reinforcement due to interlocking of stones thereby shear stress mobilization between geogrid and granular materials, due to this lateral support increases. The use of a horizontal geogrid layer sand vertical geotextile encasement offers a greater bearing capacity than vertical geogrid alone.

From the above Fig. 5, the ordinary stone column and column encased with non-woven geotextile following the similar trend up to 50 mm settlement further geotextile encasement increase the load carrying. This may be due to the initial compression of stones in the column; Once it reaches the maximum

compression, radially deformation takes place. In the case of geotextile encasement, radial confinement offers resistance. Similarly, both the high confinement systems (HC-1, HC-2) exhibit a similar trend in maximum load-carrying up to 50 mm settlements. This may be due to geogrid, and geotextile provides the maximum lateral support to stones in the column.

#### 4.2 High Encasement Effect on Load Carrying Ratio of Composite Ground

To compare the strength of each encasement of the stone column, the load-carrying capacity ratio (LCR) parameter is an express from Eq. 1 (Chenari et al. 2016), that is the maximum load carried by the ground

treated with the stone column ( $q_R$ ) to the maximum load carried by the untreated  $q_0$  (with no stone column).

$$LCR = \frac{q_R}{q_0} \quad (1)$$

Figure 6 presented the L.C.R variation with settlement and diameter of footing diameter for different stone columns. The L.C.R values are 0.61, 0.92, 2.08, 2.19 and 3.19 for OSC, GT, GD, HC-1 and HC-2 respectively at corresponding  $s/D$  (%) value of 31.7%. The minimum value of L.C.R is for the OSC and maximum L.C.R is HC-2 high confined lateral support system. From Fig. 6, OSC, GT and HC-1 similar trend is following up to the certain limit of settlement, beyond that high confined system increases significantly. This trend may be the reason is that OSC and geotextile confinement offers zero to the little amount of lateral support, once the horizontal layers in the column start resisting the lateral bulging the L.C.R values are increases. The other two cases of encasement that is vertical geogrid alone, geogrid + geotextile following the similar trend up to one point of settlement after that high confined system is shown progressive improvement of the L.C.R values. This may be geogrid offers higher modulus of elasticity than the geotextile. Similar kind of results published by the Murugesan and Rajagopal (2010), Gu et al. (2016) and Ghazavi et al. (2018).

#### 4.3 High Encasement Effect on the Axial Strain, the Radial Strain on the Stone Column

The effect of stone column various confinement systems studied in terms of the axial strain, radial strain at an applied pressure. Figure 7 presented the results of the various confinement systems at an applied pressure on the stone column. The applied pressures at 35 kPa, the settlement values are obtained as 50 mm, 50 mm, 28 mm, 47 mm and 24 mm for OSC, GT, GD, HC-1 and HC-2, respectively. Maximum settlement shown by the GT case and minimum is HC-2. The axial strain and radial strain for all cases were calculated with the dial gauges and strain gauges. The two high confined system cases show better results that are resisting the lateral bulging of the stone column. This will help us to understand the low compacted granular soils and the undrained strength of the clay soil is less than the 11 kPa can be strengthened with the help of the high confined supporting system. The further author wants to use the same kind of high confined lateral support system in the case of densified very old solid waste dump sites. This will help to increase the consolidation rate, reduce the settlement and density can be increased the composite solid waste dumpsite areas, so that land can be reclaimed for further low-level constructions. It is very evident from the Fig. 8, which is the settlement reduction ratio with the various encasement of the stone column.

The settlement reduction ratio is calculated from Eq. 2 (BIS 15284:2003: 2003) that is the ratio of settlement of treated soil ( $S_t$ ) to the settlement of

**Fig. 6** Load carrying ratio of OSC and GESC's with settlement

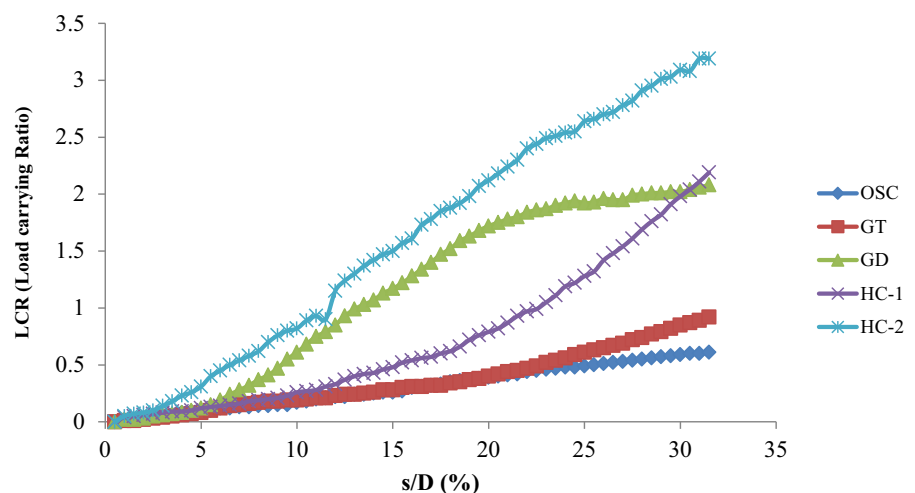


**Fig. 7** Response of the stone column with high confinement

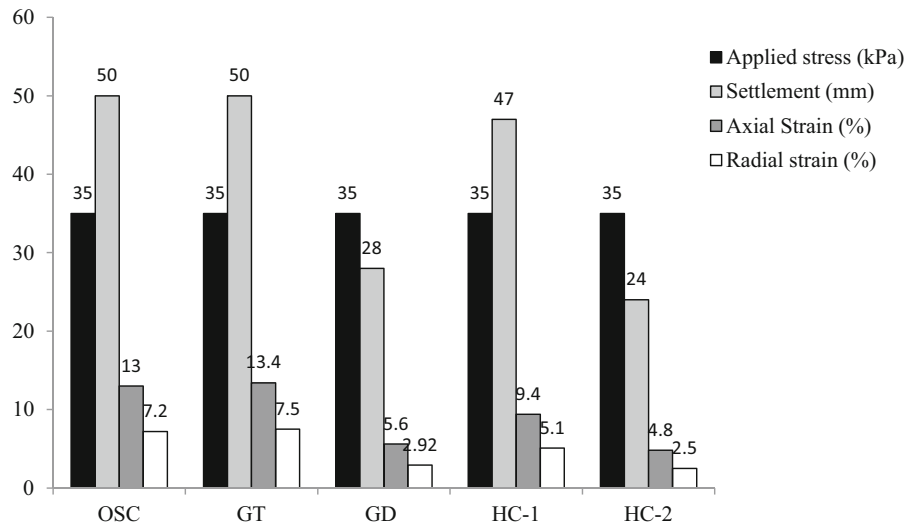
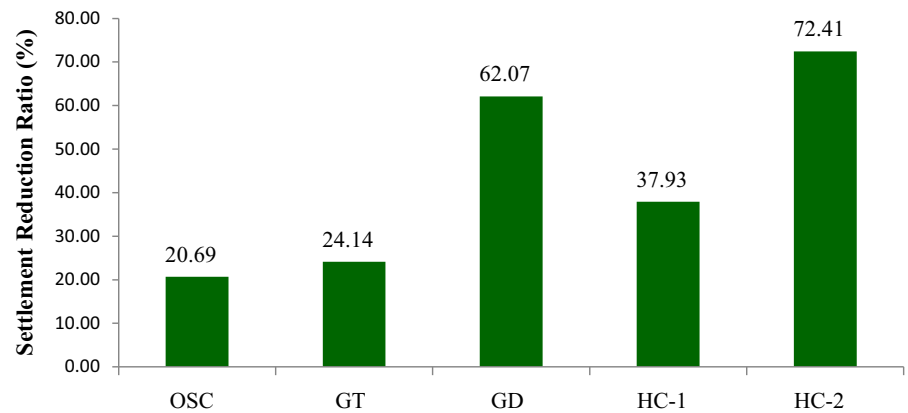


**Fig. 8** Improvement of settlement reduction ratio of OSC and GESC's



untreated soil ( $S_u$ ). It is considerably improved in case geogrid used as encasement case.

$$SRR = \frac{S_t}{S_u} \tag{2}$$

The SRR values are 20.6%, 24.14%, 62.07%, 37.9% and 72.4% of OSC, GT, GD, HC-1 and HC-2, respectively. The maximum reduction ratio is for the high confined system. Therefore it can be used for the loose granular soils, where relative compaction or relative density values are smaller and very soft cohesive soils.

#### 4.4 High Encasement Effect on Stiffness/Modulus of Subgrade Reaction of Composite Ground

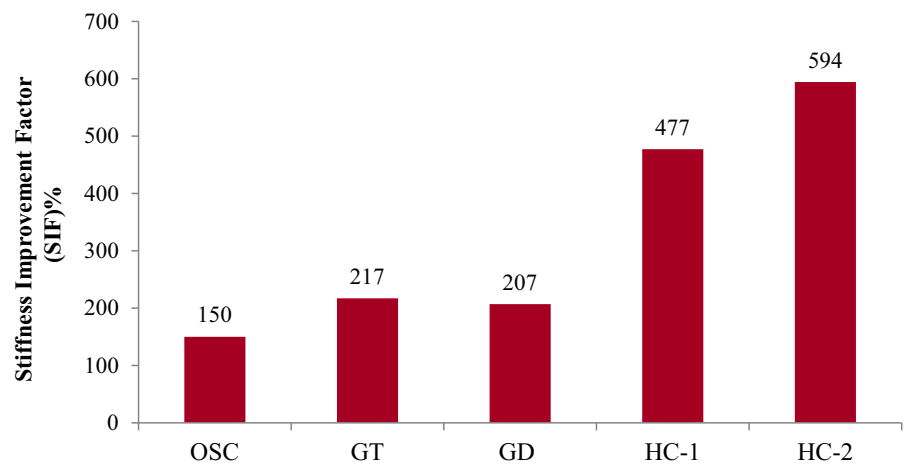
The stiffness of the composite soil is defined as load per settlement that is calculated from the load-settlement curve of the plate load test.

They are the useful parameters for designing the raft and mat foundations. The present study stone columns are encased with various materials that composite ground stiffness and stiffness improvement factor are calculated and values presented in Fig. 9 and Fig. 10. The stiffness values of the stone column encased with various geosynthetics are 7 kN/m, 17.5 kN/m, 22.2 kN/m, 21.5 kN/m, 40.4 kN/m and 48.4 kN/m of no column case, OSC, GT, GD, HC-1 and HC-2, respectively. Applied stress maximum is taken by the stone column. Different columns

**Fig. 9** Effect of encasement on stiffness of the composite ash fills



**Fig. 10** Variation of stiffness improvement factor with stone column encasement



measured the stiffness of the composite ground at the relative density of 40%, various stone columns calculated the stiffness of the composite ground; it increases from the OSC case to high confined encasement system. This may be attributed to densely compacted stones in the column, internal friction of the stones, encasement material geotextile, geogrid and a combination of horizontal geogrid layers and vertical encasement. The stiffness improvement factor (SIF) calculated using expression 3 (Chenari et al. 2016) and the same thing presented in Fig. 10.

$$SIF = \frac{k_{impr} - k_{unimpr}}{k_{unimpr}} \times 100 \quad (3)$$

#### 4.4.1 Modulus of Subgrade Reaction

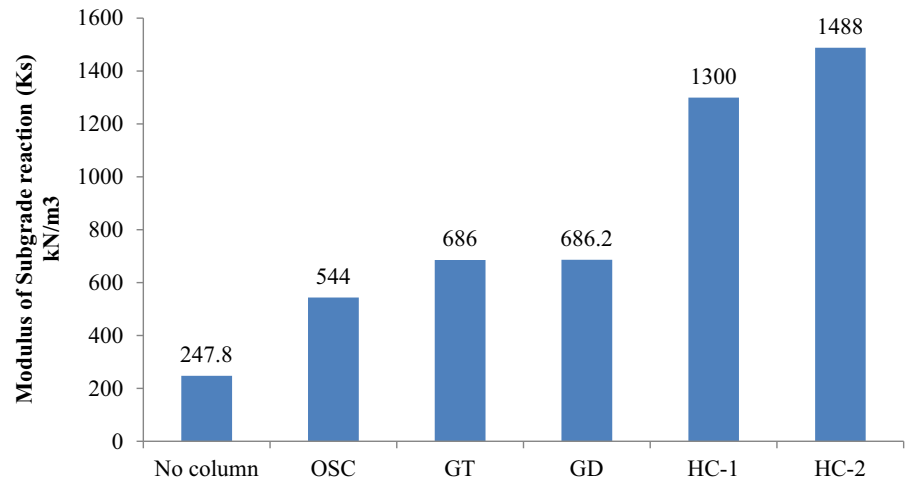
The modulus of subgrade reaction is a conceptual relationship between soil pressure and deflection

which is used vastly in the analysis of foundation members. It is useful in pile subjected to lateral load, strip footings, mats and other types of foundation members design. The modulus of subgrade reaction ( $K_s$ ) is obtained from Eq. 4, it can be defined as the initial slope of the applied pressure ( $\Delta\sigma$ ) to the settlement ( $\Delta\delta$ ) of the plate load test curve.

$$K_s = \frac{\Delta\sigma}{\Delta\delta} \quad (4)$$

The present study on ash fills are reinforced with the high encased stone columns, modulus of subgrade reaction is calculated using the following Eq. 4 (Bowles 1968).  $K_s$  is obtained from the plot of pressure versus deformation (initial slope of the pressure and deformation curve). The modulus of subgrade reaction of the ash fills treated with the stone columns presented in Fig. 11. Referring to Fig. 11,  $K_s$

**Fig. 11** Improvement of modulus of subgrade reaction with different stone column encasement



for untreated, treated ash fills with granular stone columns and treated with the various encasement systems were 247.8, 544, 686.2, 686, 1300 and 1488 kN/m<sup>3</sup>, respectively. These values are lower side as compared to the clay soil treated with the granular column jacketing with tubular wire mesh, metal bridging rod and concrete plug by Black et al. (2007). The variation in values may be initial loading on the composite bed. Also, observe the high confined system gives higher values that are contributed by the presence of double geosynthetics encasement.

#### 4.5 Slope Reinforced With the Encased Stone Column

Civil engineers (geotechnical) have a concern about the stability of steep slopes and landslides. Various methods were used in the past to stabilize the slopes and landslides, such as retaining walls, breast walls, piles, geocells and woven geotextiles. They may be used to strengthen and increase the factor of safety of slope stability. Stone columns are used at the base of the embankment to increase stability. Naderi et al. (2018) and Vekli et al. (2012) worked on slopes reinforced with ordinary stone columns both experimentally and numerically verified that they are a potential alternative for slope stabilization. The present study slope is made using the pond ash at a slope angle of 45°. Geogrid encased stone column created below the circular footing of 100 mm diameter with an offset of 100 mm from the edge of the slope. The load applied through the circular footing on slope reinforced with an encased stone column. The results are

plotted in Fig. 12 that is applied for stress and settlement. Referring to Fig. 12 the applied stress steadily increases up to 260 kPa at a correspondingly 72 mm settlement. Slope failure yielding point at 260 kPa, further applied load on the slope, load-carrying capacity increases to 450 kPa even after post-failure. This may be due to the entire load carried by the stone column alone after the slope failure. This may be used full where steep slopes are made of granular soils and soil sliding can be arrested with the help of encased stone columns. This may restrict the complete failure of the slopes and reduce the damage. Failure patterns of the various encased stone columns presented in Fig. 14.

#### 4.6 Failure Patterns of the Stone Column

The failure mode of a single column loaded over an area significantly depends on the length of the column. The length of the column is greater than the 4 times its diameter, the column will fail in bulging (Barksdale and Bachus 1983; BIS 15, 284: 2003). As for the maximum lateral deformation takes place at a depth of 2d (d is the diameter of the stone column) from the surface. Many research scholars studied the failure mode of a single column in soft clay soils (Murugesan and Rajagopal 2010). In the present study, the encased stone column failure observed at maximum load application in loosely compacted (relative density is 40%) pond ash. Referring to Fig. 13a is the failure of the geogrid encased stone column, the maximum lateral deformation took place at a distance of d–3d from the surface. Whereas Fig. 13b is high confined

**Fig. 12** Load—settlement behavior of slope reinforced with GESCs (GDS case)

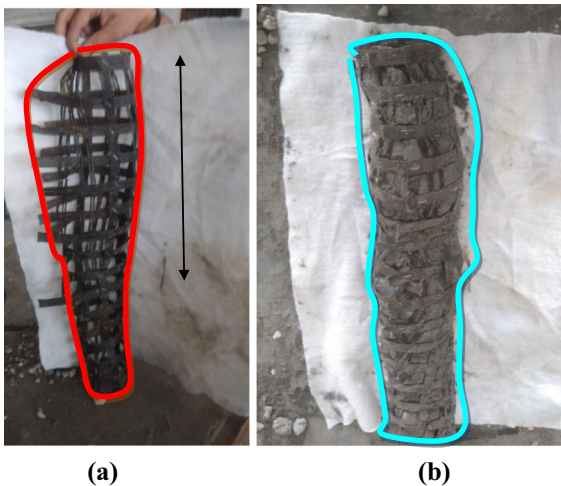
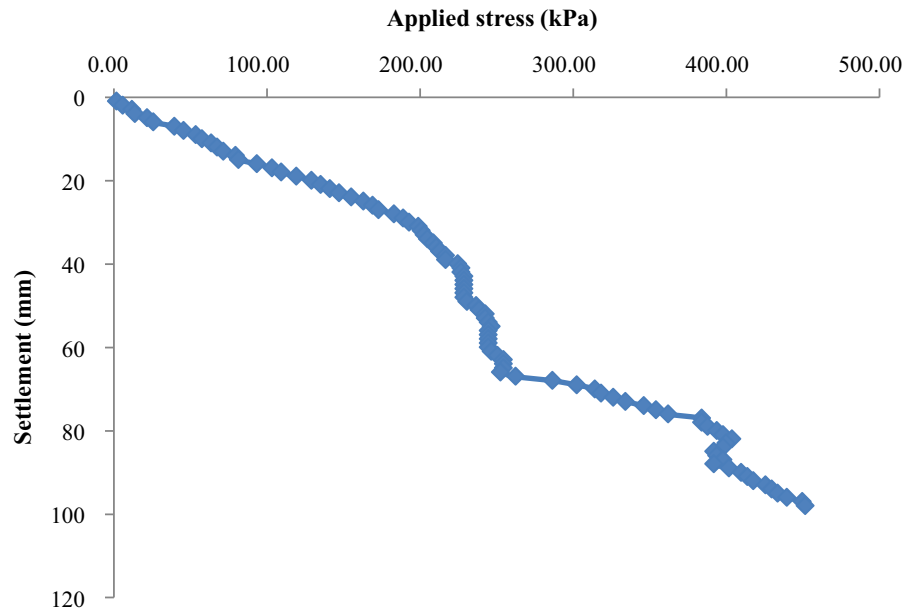


**Fig. 13** Failure behavior of stone column encased with **a** geogrid (GD), **b** high confined (HC-2)

encased stone column, lateral deformation is slightly increased size of the bulging is smaller at the same distance, beyond which it almost remains the constant diameter. This is due to high lateral support by the geogrid and geotextile.

Failure of slope reinforced with geogrid encased stone column presented in Fig. 14. The bulging of the stone column is at a distance of  $d$ – $2d$ , this may be the reason the offset distance from the edge is smaller, due to the smaller passive pressure the bulging starts from

the distance ‘ $d$ ’, and it continues to till  $2d$ , beyond that distance size of the column, is remained same.

## 5 Experimental Modeling Considerations

The main issue of all the laboratory experiments is scaling. The scale ratio is any linear dimension of the prototype to the equivalent dimension of the model. From the literature scale, ratio slightly varies the diameter of the stone column and aggregate size. The diameter of the stone column in practice ranging from 0.6 to 1.0 m and the size of the aggregates are 12 to 75 mm (Barksdale and Bachus 1983). The scale representation of the prototype to the model was one–eighth (Black et al. 2007). In the present study, the diameter of the stone column in the model tests as 80 mm. The scale ratio becomes 7 and 12. Because of  $L/D$  ratio to be 6 in the model tests, the column length for the 80 mm diameter test column will be 480 mm. From the literature, the particle size ( $d_s$ ) of aggregates to be filled in the column varies between 12 and 75 mm in the prototype stone columns  $d_p/d_s$  ratio varies between 12 and 40. The particle size of the aggregates in the model stone columns was kept as 2–6 mm corresponding to  $d_p/d_s$  ratio ranging between 9 and 25. It is therefore considered that the scale effects are minimized in the present study.

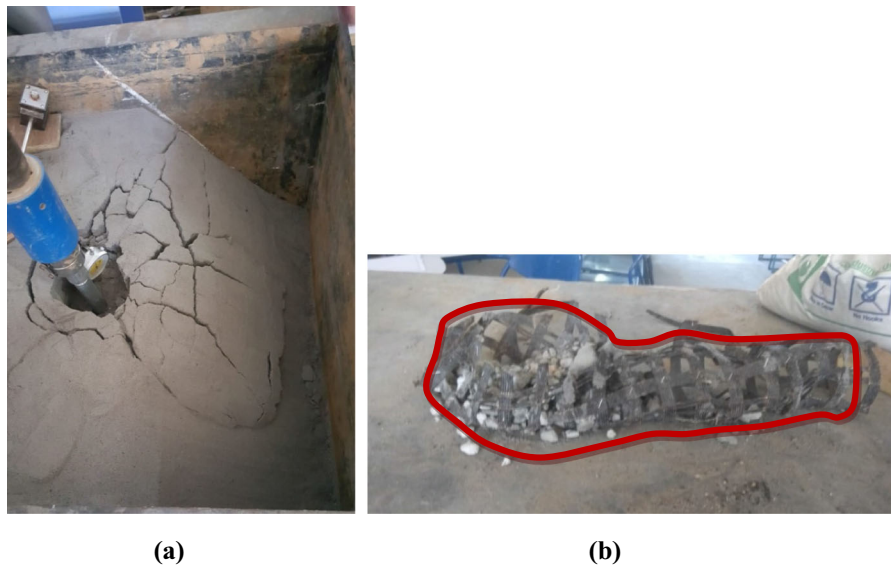


**Fig. 14** **a** Failure of the slope reinforced **b** Failure of geogrid encased stone column

The geotextile and geogrids are chosen for strengthening the SC (stone column) is the main task in laboratory model tests concerning the scale effect concept and similarity analysis rules. Since the material unit weight of the model and fields are very similar, it is concluded that the stiffness of reinforcing material should be reduced by power two of the ratio of model size to field size. While for selecting the encasement of stone columns, consider the opening size of the geogrid is smaller than the average aggregate size, so that the column aggregates cannot pass through it and secondly, considering the stiffness of the encasement. Murugesan and Rajagopal (2010), Ghazavi and Afshar (2018) used the woven and non-woven geotextiles stiffness is up to 10,000 kN/m. Scaling laws proposed by Iai (1989), the relationship between field-scale reinforcement stiffness ( $K_f$ ) can be calculated as  $K_f = K_m \cdot l^2$ , where  $l$  is the model scale. In the present work, the model scale assumed 1/12. The stiffness of encasement in the model tests of the current study should be less than with the full-scale condition ( $K_f = 150 k_m$ ). Therefore, in the present research work 80 mm diameter stone column, two types of encased materials were used, nonwoven geotextile (GT) and biaxial polyester geogrid (GD/GL) with secant stiffness of 6.8 kN/m and 33 kN/m, respectively.

### 5.1 Numerical Modelling

A numerical model was developed using a Plaxis FE (finite element) technique to validate the stone columns placed in ash fills. The model was set 15-node triangular mesh elements to provide the optimum distribution of stress- strains and hence magnify the level of accurateness in the data generated. In model fine mesh generation was used for the global coarseness, while it was refined twice in places where high stresses and displacements were likely to occur. During this investigation, a circular foundation was taken and each stone column and surrounding soil (under the footing) bear uniform settlement. At the bottom of the mesh, the model was fixed support, and roller supports were used on the vertical boundaries; therefore, the horizontal and vertical stress concentrations were eliminated. The popular constitutive law for soils of Mohr–Coulomb was used to analyze the stone columns and the ash fills and linear elastic behavior was used for the reinforcing materials, details of the parameters used in numerical analysis are presented in Table 5. An axisymmetric model was applied for a stone column with a uniform radial cross-section and loading scheme around the central axis where the deformations and stresses are assumed to be identical in the radial direction. From literature various researchers are studied the improvement with the stone columns when the area replacement ratio is less

**Table 5** Material properties used in numerical analysis (Plaxis)

Material property	Ash fill	Aggregates (column fill material)	Geotextile	Geogrid
Material model	Mohr–coulomb	Mohr–coulomb	Linear elastic	Linear elastic
Unsaturated unit weight, $\gamma$ , kN/m <sup>3</sup>	11	18	–	–
Saturated unit weight, $\gamma_{\text{sat}}$ , kN/m <sup>3</sup>	14	20	–	–
Modulus of elasticity, EkN/m <sup>2</sup>	200	40,000	–	–
Poissons ratio, $\nu$	0.3	0.2	–	–
Cohesion, $c$ , kN/m <sup>2</sup>	2	1	–	–
The angle of internal friction, $\phi$	30	44	–	–
Dilation angle, $\varphi$	–	14	–	–
Secant stiffness, kN/m	–	–	1000	4500

than 10%, for the current study, the area replacement ratio ( $A_s$ ) was taken less than 10%. According to a program reference manual, an interface ratio of 0.67 was used for the interface between reinforcement and stone column material. All analysis was performed by applying displacement increments using a prescribed displacement method to simulate the rigid footing condition on top of the column as used in tests. To remove the effects of element size and boundary conditions in the numerical analysis, sufficiently extended boundaries with fine mesh discretization were considered.

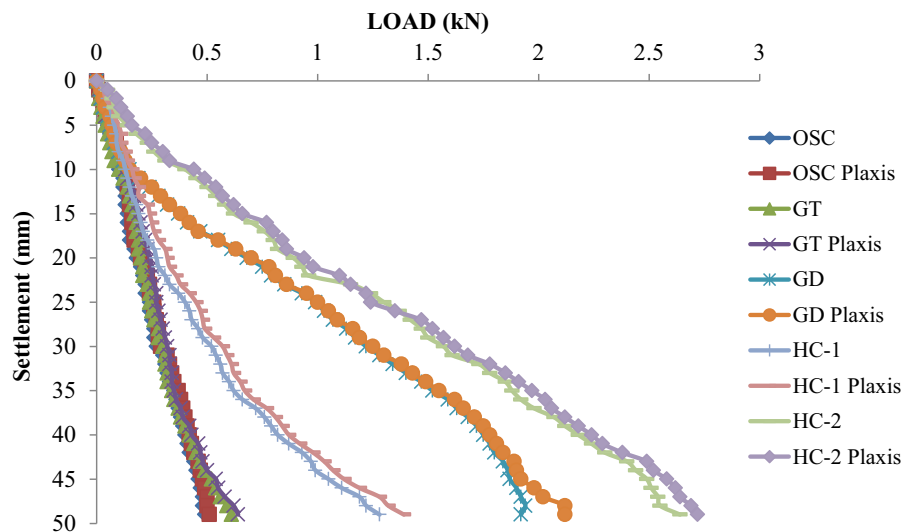
Figure 15 shows the comparison of load–settlement results between the experimental model tests and numerical analysis on OSC, GT, GD, HC-1 and HC-2 based on unit cell concept of full encasement of the

stone column. Small deviation (regression coefficient  $R^2$  is 0.993) between the experiment and plaxis analysis shown in high encasement cases; This may be due to numerical analysis parameters being slightly higher side, interface element mesh size, and interface factor. That is interfaces between column–ash fill, geotextile–ash fill, geogrid–ash fill and horizontal grid layers–aggregates in the column, resulted in larger settlements especially higher vertical loads.

## 5.2 Effect of High Encasement on Lateral Deformation

Lateral deformations were observed under the unit cell condition using the Plaxis model. The study shows that a bulging zone turns out a maximum lateral

**Fig. 15** Experimental results validation with plaxis numerical analysis



deformation in the surrounding area of the ground surface, the magnitude of which is in effect vertical load and time-dependent. For a particular depth, the column lateral deformation was found to increase sharply 0–15 mm and thereafter gradually stabilized. A negligible small lateral deformation was formed near the column top because high vertical deformation is predominant (primarily compression).

From Fig. 16 OSC case the lateral deformation is much higher than the high encased system that is HC-2, GT and HC-1. The amount of lateral deformation can be reduced up to 92% and 74% in the case of HC-2 and HC-1 encasement system with a comparison of OSC case. The lateral deformation is considerably reduced with the high encasement system even in loose ash fills. This system of high encasement can be applied to the low consolidated, decomposed solid waste dump sites and in landfill sites as well. Due to the higher tensile strength and stiffness of geogrids and geotextiles, the stone column and surrounding soil (composite) ground increases its stiffness thereby increase the bearing capacity and reduce the vertical settlement.

### 5.3 Failure Patterns in High Encased sc’s (Numerical Modeling)

From the experimental and numerical analysis, bulging failure mode directs the single stone column.

Many of the previous researchers confirm the bulging failure in soft clay soil occurs at a depth of  $D-2D$  from the column starting point. In case of the loose ash fills where it is having a relative density is 40% the depth of bulging is at a  $2D$  distance as shown in Fig. 17a in case of the ordinary stone column. Remaining cases due to the high encasement, the lateral bulging failure controlled (Fig. 17b, c) and bear the relatively higher load at low vertical settlement.

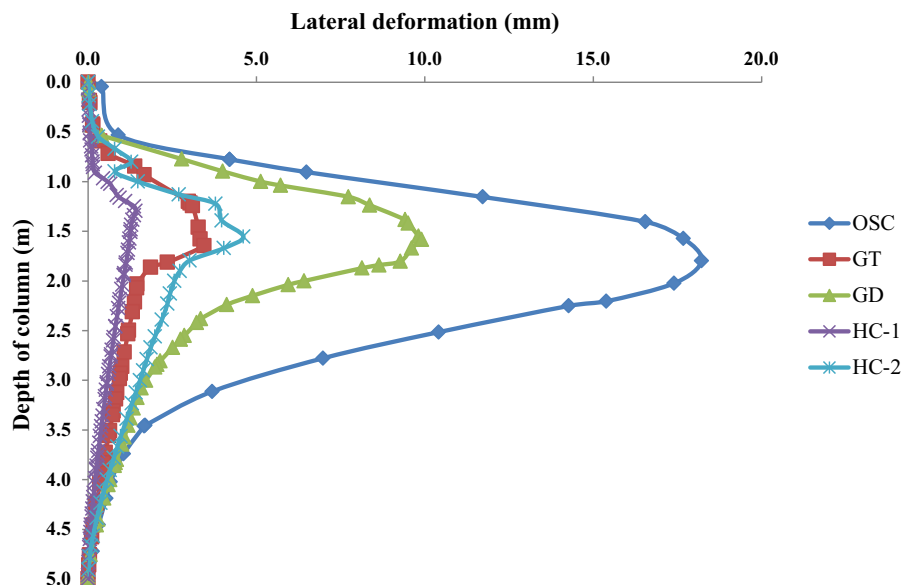
With increasing the strength of reinforcement stiffness in the form of horizontal geogrids at every  $d$  (diameter of SC) distance and vertical encased geotextile, the ultimate capacity and stiffness of the column increased. In case of slopes reinforced with the encased SC, the bulging failure took place at the factor of safety of 1.04. As shown in Fig. 17d. it may be the not stable condition. Further, the author may be interested to increase the slopes (1:1.5, 1: 2 and 1: 2.5) with the inclined high encased stone columns.

## 6 Conclusions

The present study on loose ash fills treated with stone columns, circular footing—200 mm dia plate, 80 mm dia. of the stone column and it is encased with GT, GD, HC-1 and HC-2 the following conclusions are drawn.

- The load-carrying capacity and stiffness of the stone column increased with the vertical

**Fig. 16** Lateral deformation of OSC and GESC’s



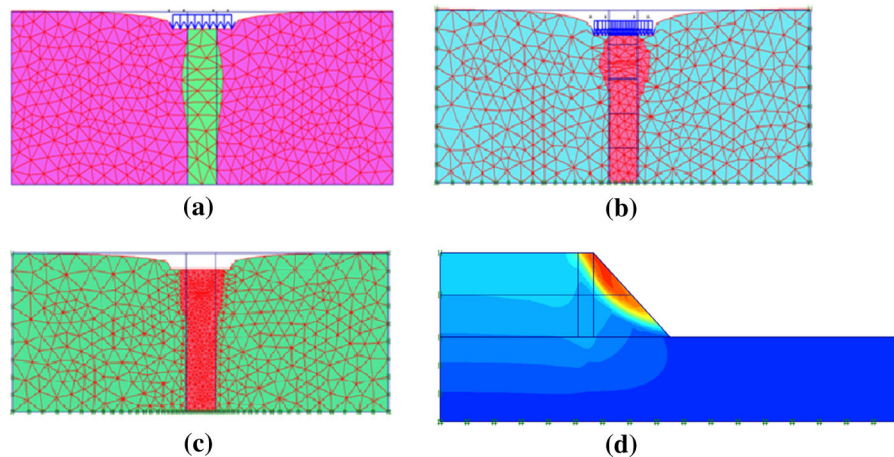


**Fig. 17** Deformed mesh of stone columns **a** OSC, total displacement = 100 mm, **b** HC-1, high confined SC, displacement = 37 mm, **c** HC-2 high confinement, displacement = 9 mm **d** slope reinforced with SC, factor of safety is 1.04

encasement of geotextile, geogrid and the combination of both vertical and horizontal layers. Higher confining encasement provides tensile stiffness and low creep.

- The HC-1 and HC-2 used as a higher confinement system at loose compacted ash fills. Both the confinement system yields better results in load carrying capacity, stiffness of the column, and modulus of subgrade reaction. The L.C.R values are 0.61, 0.92, 2.08, 2.19 and 3.19 for OSC, GT, GD, HC-1 and HC-2, respectively, over untreated soils.
- The SRR values are 20.6%, 24.14%, 62.07%, 37.9% and 72.4% of OSC, GT, GD, HC-1 and HC-2, respectively. The maximum reduction ratio is for the high confined system.
- The stiffness values of the stone column encased with various geosynthetics are 7 kN/m, 17.5 kN/m, 22.2 kN/m, 21.5 kN/m, 40.4 kN/m and 48.4 kN/m of untreated, OSC, GT, GD, HC-1 and HC-2, respectively.
- $K_s$  (modulus of subgrade reaction) for untreated, treated ash fills with granular stone columns and treated with the various encasement systems are 247.8, 544, 686.2, 686, 1300 and 1488 kN/m<sup>3</sup> of untreated, OSC, GT, GD, HC-1 and HC-2, respectively.
- The use of geotextile and the geogrid combination can restrict lateral deformation due to its tensile strength. The amount of lateral deformation can be reduced up to 92% and 74% in the case of HC-2

and HC-1 encasement system with a comparison of the OSC case. Therefore, it can be applied to the ash fill, demolition debris and silty clay fills.

- The failure mode of the column is in bulging. Higher confinement of GESC controls bulging failure. The predominate failure of the GESC took place within the range of 1D to 3D (D—diameter of the column) depth of the column from the surface. This confirms with numerical analysis as well. To maximize the effect of confinement, it should be suggested that encasement be provided at least 4D.
- The slopes (moderately steep) of ash fills reinforced with the OSC and GESC under the footing improves its stability and bearing pressure. Slope failure yielding point is 260 kPa at 72 mm vertical settlement, post failure load-carrying capacity continues upto 450 kPa. This explains the massive failures (landslide) of slopes can be controlled.
- Numerical analysis validation is 10% to 15% deviation for higher confinement system. It may be due to higher interaction factor, interface between encasement material–soil, column fill material–encasement and material properties.

**Acknowledgements** The author(s) are grateful to the DAV Institute of Engineering & Technology, who allowed us to work in the laboratory, lab technicians and students. The author(s) are grateful to the respected reviewers for their valuable suggestions for improving the presentation of this paper.

## References

- Alexiew D, Brokemper D, Lothspeich S (2005) Geotextile encased columns (GEC): load capacity, geotextile selection and pre-design graphs. In: proceedings of Geo Frontiers 2005, Austin, Texas, United States, pp. 497–510
- Ali K, Shahu JT, Sharma KG (2014) Model tests on single and groups of stone columns with different geosynthetic reinforcement arrangement. *Geosynth Int* 21(2):103–118
- Ambily AP, Gandhi SR (2007) Behaviour of stone columns based on experimental and FEM analysis. *J Geotech Geoenviron Eng*. 133(4):405–415
- Amini R (2016) Physical modelling of vibro stone column using recycled aggregates. Doctoral dissertation, University of Birmingham
- Ayothiraman R, Soumya S (2015) Model tests on the use of tyre chips as aggregates in stone columns. *Proc Inst Civil Engineers-Ground Improvement* 168:187–193
- Bairagi K, Murali G, Reddy SN (2012) Efficacy of stone columns in fly ash area—A case study. In: Proceedings of Indian Geotechnical Conference., Kochi, Dec 15th–17th, 2011, pp. 995–998
- Barksdale RD, Bachus RC (1983) Design and construction of stone columns, FHWA / RD-83/026. Federal Highway Administration, Washington, D.C. doi: FHWA / RD-83/027
- BIS: 2386(4):1963 Methods of Test for Aggregates for Concrete- Mechanical Properties, Reaffirmed. Dec 2016
- BIS: 15284 (2003) Design and construction for ground improvement—guidelines. Part 1. Bureau of Indian Standards, New Delhi
- BIS: 2720 (13) (1986) Methods of test for soils, direct shear test. Bureau of Indian Standards, New Delhi
- BIS: 2720 (17) (1986) Methods of test for soils, laboratory determination of permeability. Bureau of Indian Standards, New Delhi
- BIS: 2720 (4) (1985) Methods of test for soils, grain size analysis. Bureau of Indian Standards, New Delhi
- BIS: 2720 (8) (1985) Methods of test for soils, Determination of water content – dry density relation using heavy compaction test. Bureau of Indian Standards, New Delhi
- Bowles JE (1968) Foundation analysis and design, 5th edn. McGraw Hill Education India Pvt Ltd, New York
- Black JA, Sivakumar V, Madhav MR, Hamill GA (2007) Reinforced stone columns in weak deposits: laboratory model study. *J Geotech Geoenviron* 133(9):1154–1161
- Cengiz C, Guler E (2018) Seismic behavior of geosynthetic encased columns and ordinary stone columns. *Geotext Geomembr* 46:40–51
- Chenari RJ, Fard MK, Chenari MJ, Sosahab JS (2016) Physical and numerical modeling of stone column behavior in loose sand. *Int J Civ Eng*. <https://doi.org/10.1007/s40999-017-0223-6>
- Dash SK, Bora MC (2013) Influence of geosynthetic encasement on the performance of stone columns floating in soft clay. *Can Geotech J* 50:754–765
- Debnath P, Dey AK (2017) Bearing capacity of geogrid reinforced sand over encased stone columns in soft clay. *Geotext Geomembr* 45:653–664
- Demir S, Mokarram FR, Ozener P (2016) The sustainable design of granular columns based on laboratory model tests. *Geo-Chicago 2016 GSP* 271, pp. 893
- Fattah MY, Zabar BS, Hassan HA (2016) Experimental analysis of embankment on ordinary and encased stone columns. *Int J Geomech* 16(4):04015102
- Gandhi SR, Dey AK, Selvam S (1999) Densification of pond ash by blasting. *J Geotech Geoenviron* 125(10):889–899
- Ghazavi M, NazariAfshar J (2013) Bearing capacity of geosynthetic encased stone columns. *Geotext Geomembr* 38:26–36
- Ghazavi M, Yamchi AE, Afsar JN (2018) Bearing capacity of horizontally layered geosynthetic reinforced stone columns. *Geotext Geomembr* 46:312–318
- Gniel J, Bouazza A (2009) Improvement of soft soils using geogrid encased stone columns. *Geotext Geomembr* 27(3):167–175
- Gniel J, Bouazza A (2010) Construction of geogrid encased stone columns: a new proposal based on laboratory testing. *Geotext Geomembr* 28(2010):108–118
- Greenwood DA (1970) Mechanical improvement of soils below ground surfaces. In: Proc. ground engineering conference, Institution of Civil Engineers, London, pp. 11–22
- Gu M, Zhao M, Zhang L, Han J (2016) Effects of geogrid encasement on lateral and vertical deformations of stone columns in model tests. *Geosynth Int* 23(2):100–112
- Hassan AK, Alturffy UAS (2015) Stability analysis of side slope by using stone column and tieback support. *Int J Sci Eng Res* 5(9):1837–1844
- Hughes JMO, Withers NJ (1974) Reinforcing of soft cohesive soils with stone columns. *Ground Eng* 1(3):42–49
- Iai S (1989) Similitude for shaking table tests on soil-structure-fluid model in 1g gravitational field. *Soils Found* 29(1):105–118
- Malarvizhi SN, Ilamparuthi K (2007) Comparative study on the behavior of encased stone column and conventional stone column. *Soils Found* 47(5):873–885
- Mazumder T, Rolaniya AK, Ayothiraman R (2018) Experimental study on behaviour of encased stone column with tyre chips as aggregates. *Geosynth Int* 25(3):259–270
- Miranda M, Da Costa A (2016) Laboratory analysis of encased stone columns. *Geotext Geomembr* 44(3):269–277
- Mohapatra SR, Rajagopal K, Sharm J (2016) Direct shear tests on geosynthetic encased granular column. *Geotext Geomembr* 44(2016):396–405
- Murugesan S, Rajagopal K (2010) Studies on the behavior of single and group of geosynthetic encased stone columns. *J Geotech Geoenviron* 136(1):129–139
- Naderi E, Asakereh A, Dehghani M (2018) Bearing capacity of strip footing on clay slope reinforced with stone columns. *Arab J Sci Eng* 43(10):5559–5572
- Prasad SSG, Satyanarayana PVV (2016) Improvement of soft soil performance using stone columns improved with circular geogrid discs. *Indian J Sci Technol* 9(30):1–6
- Rao GV, Pothal GK (2009) Improvement of pond ash with prefabricated vertical drain. In: Indian geotechnical conference, Guntur
- Reddy CS, Mohanty S, Shaik R (2018) Physical, chemical and geotechnical characterization of fly ash, bottom ash and municipal solid waste from Telangana state in India. *Int J Geo Eng* 9:1–23

- Salem ZB, Frikha W, Bouassida M (2017) Effects of densification and stiffening on liquefaction risk of reinforced soil by stone columns. *J Geotech Geoenviron Eng* 143(10):1–6
- Shahverdi M, Haddad A (2019) Use of recycled materials in floating stone columns. *Proc Inst Civil Engineers-Construction Mater*. <https://doi.org/10.1680/jcoma.18.00086>
- Sharholy M, Ahmad K, Mahmood G, Trivedi RC (2008) Municipal solid waste management in Indian cities—a review. *J Waste Manag* 28:459–467
- Shivashankar R, Dheerendra Babu MR, Nayak Sitaram, Manjunath R (2010) Stone columns with vertical circumferential nail. Laboratory model study. *Geotech Geo Eng* 28:695–706
- Singh S, Singh SK (2018) Geotechnical characterization and WRCC for spatially varied pond ash within as ash pond. *Indian Geotech J*. <https://doi.org/10.1007/S40098-018-0340-4>
- Trivedi A, Sud VK (2007) Settlement of compacted ash fills. *Geotech Geol Eng* 25:163–176
- Vekli M, Aytakin M, Ikizler SB, Calik U (2012) Experimental and numerical investigation of slope stabilization by stone columns. *Nat Haz* 64:797–820
- Wu CS, Hong YS (2009) Laboratory tests on geosynthetic encapsulated sand columns. *Geotext Geomembr* 27(2):107–120
- Yoo W, Kim B, Cho W (2015) Model test study on the behavior of geotextile-encased sand pile in soft clay ground. *KSCE J Civ Eng* 19(3):592–601

**Publisher's Note** Springer Nature remains neutral with regard to jurisdictional claims in published maps and institutional affiliations.